Einselection and the quantum to classical transition in quantum dots

2005 J. Phys.: Condens. Matter 17 S1017

(http://iopscience.iop.org/0953-8984/17/13/001)

INSTITUTE OF PHYSICS PUBLISHING JOURNAL OF PHYSICS: CONDENSED MATTER

J. Phys.: Condens. Matter **17** (2005) S1017–S1036 doi:10.1088/0953-8984/17/13/001

Einselection and the quantum to classical transition in quantum dots

David K Ferry, Richard Akis and Jonathan P Bird

Department of Electrical Engineering and Center for Solid State Electronics Research, Arizona State University, Tempe, AZ 85287-5706, USA

E-mail: ferry@asu.edu

Received 9 August 2004, in final form 25 August 2004
Published 18 March 2005
Online at stacks.iop.org/JPhysCM/17/S1017

Abstract

Recent work on the role of decoherence in quantum physics has suggested that the quantum to classical decay is governed by a discrete set of pointer states, which are quite stable and uncoupled from other states in the system. We show that the conductance oscillations exhibited by open quantum dots are governed by a discrete set of stable quantum states which have the properties of the pointer states, and which are closely related to trapped classical orbits in the open dot. These states are essentially classical in nature, as evidenced by their energy level spacing, and their decay is apparently in the environment as opposed to within the dots.

(Some figures in this article are in colour only in the electronic version)

1. Introduction

The description of a quantum dot can be applied to a great many types of structure, some of which are defined by physical characteristics, such as self-assembled dots [1], and others of which are defined through lithography. This can either be an etched structure [2], or achieved by the imposition of a self-consistent potential which is applied through a set of confining gates [3]. Indeed, the range of these different types of structures is sufficiently large that no single review can hope to cover them. Yet, the application of quantum dots has become important in an equally wide range of technical fields, for both optical and electronics applications. For that reason, we limit ourselves to gate-defined examples which have proven useful for the investigation of new phenomena in transport physics, and which promise a new understanding of quantum information science, particularly the transition from quantum to classical behaviour through decoherence.

One of the earliest gate-defined lateral quantum dots was fabricated on a GaAs/AlGaAs heterojunction, in which a quasi-two-dimensional electron gas is formed on the GaAs side of

the hetero-interface [3]. In this structure, depletion under a set of metal gates formed a quantum wire between the gates, and small extensions of the gates created two quantum point contacts (QPC) through which the current flowed into, and out of, the dot. These QPCs were biased to the point that they provided a tunnelling barrier, so that transport was by single-electron tunnelling, and the quantum energy levels could be studied. It has been assumed generally that tunnelling barriers were required to maintain the quantization within the dot, and that the levels would be broadened to the classical level if these dots were 'opened' [4], a prediction that seemed to be supported by early measurements [5, 6]. We now know this is not the case, and the degree to which an individual quantum state is broadened depends upon how it couples to the external world (the environmental system outside the dot) [7–10]. As a consequence, these open dots remain quantum objects, a result that is useful if they are to be incorporated in any new type of information processing.

In the early studies mentioned above, the transport properties of quantum dots were investigated under conditions where the dot was only *weakly* coupled to its reservoirs, and where current flow was made possible by the *tunnelling* of electrons through the dot. In experiments of this type, the resulting transport is critically influenced by two different effects. The first of these is the finite *charging energy*, associated with the addition of a single electron to the dot. This gives rise to the Coulomb blockade of current. The other important effect is the energy quantization that is induced when the dots are used to confine electrons on a size scale that may even approach their (Fermi) wavelength.

In *open* quantum dots, which are coupled to their reservoirs by means of waveguide leads, however, it might be expected that the charge fluctuations which wash out the Coulomb blockade should also obscure the signatures of this quantum structure. In practice, however, this turns out to be incorrect, and it can even be argued that the shell structure is made *more robust* by the presence of the dot–reservoir coupling! Many states are washed out, though, and it is the remaining states that provide a new insight into the fundamental quantum physics. It is the understanding of this important new physics which is the subject of this paper.

2. Einselection

The manner in which quantum states of a system evolve into classical states has been a point of significant discussion in quantum measurement theory for a relatively long time [11]. In particular, open quantum systems interact with their environment, which is often taken to be a bath or reservoir, but also may be the measurement system itself. The output of a measurement is presumed to be classical in nature. The manner in which the quantum properties of the system are revealed in the classical results of the measurement, as well as the manner in which these quantum properties evolve into intrinsic classical properties, have been the focus of investigation since the formulation of quantum theory. One interpretation, which explicitly includes the coupled systems, is that of decoherence [12]. Decoherence is thought to be an important part of the measurement process, especially in selecting the classical results; that is, in passing from the quantum states to the measured classical states of a system [13]. However, the description (and interpretation) of the decoherence process has varied widely. A key point is that the interaction of the system upon the environment, as well as the interaction of the environment upon the system, is important. Zurek has proposed that the interaction of the system with the environment leads to a preferred, *discrete* set of quantum states, known as *pointer* states, which remain robust, as their superposition with other states, and among themselves, is reduced by the decoherence process [14]. In general, any quantum system interacts with external degrees of freedom, which are representative of the environment in which the quantum system is embedded. This interaction is important if the properties of

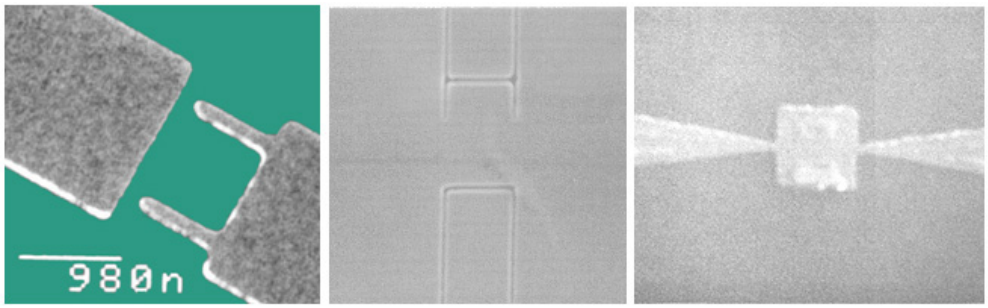

Figure 1. On the left is a dot formed by depletion under two metal gates [19], while the centre dot is formed by isolating the various regions with an etched trench to form gates in the plane of the dot [18]. On the right the entire dot has been isolated by etching away material [46]. All show the same generic behaviour, although the details are specific to each dot.

the quantum system are to be observed in the environment. This interaction, though, causes decoherence, which results in the loss of 'purity' of the states in the quantum system. Not all the states in the quantum system are equally susceptible to this, however, and there remains a smaller set of initial states that is relatively robust with respect to the interaction with the environment. These are the pointer states, and their existence is a universal property of the quantum system [15]. This decoherence-induced selection of the preferred pointer states was termed *einselection* [12]. Recently, it has been argued that the pointer states must be a continuous set of states [16]. In addition to the pointer states, there exists a sea of states that are heavily damped by the decoherence process. If the pointer states constitute a discrete set, then their robustness with respect to decoherence should make it possible to detect them in a measurement process among all the heavily damped states. However, if the pointer states constitute a continuous set, then not only would their detection in measurement be impossible, but so would any remotely precise measurement on a quantum system with a classical measuring apparatus.

Recently, we pointed out that an open quantum dot, in which the coupling to the environment is mediated by a pair of quantum point contacts, is exactly a system in which the properties of pointer states are observable [17]. In these open quantum dots, a discrete set of (pointer) states is selected, which provide a measurable conduction oscillation, and which are orthogonal to the majority of quantum states in the system. These dots are realized by applying depletion potentials to lithographically defined gates, as discussed above. These gates provide lateral confinement of a quasi-two-dimensional electron gas formed at the interface of, e.g. a GaAs/AlGaAs heterostructure (figure 1), but studies in other heterostructures give equivalent results [18]. The confinement results in a sub-micron-sized ballistic cavity that is coupled to its environment through the quantum point contacts. Conductance through these dots is governed by the transmission and reflection of waves originating in the external environment. Variation of either a normal magnetic field, or the confining potential of the quantum dot itself (by means of gate voltages), produces quasi-periodic conductance oscillations. The oscillations occur as the Fermi energy is pushed through the energy levels of the pointer states, so that they are observable in the conductance measured in the environment.

3. Fluctuations in dots

Quantum dots have been studied significantly over the past few years. Our interest is for the case in which the dots are *open* and relatively strongly coupled to the environment. In most of the

earlier studies, there was considerable effort expended to try to establish that the basic behaviour of these ballistic quantum dots was governed by *universal* properties that were *generic* in nature and independent of the specific properties of the individual dots. In fact, averaging over, e.g. the gate voltage, was used to remove the quasi-periodic fluctuations in order to reveal what was believed to be a chaotic background. In fact, this process removed the significant signatures of what we now believe to be the pointer states. In principle, the underlying physics of the ballistic quantum dots is described by characteristics that are dependent upon the individual dot under study, so that *there is a universal behaviour that is characteristic of such dots*, but it is not the generic behaviour described by the pseudo-chaotic mathematics of these previous studies. Instead, the underlying properties, and the characteristic transport through the dots, is governed by the basic *regular* nature of the semi-classical orbits in the dot [20]. This regular nature is observed as reproducible fluctuations.

In these dots, the transport is dominated, at low temperature, by reproducible fluctuations which are observed as either a magnetic field, or the gate voltage applied to the dots, is varied. These fluctuations exhibit quasi-periodic oscillations, whose nearly single frequency character is easily discernible in the correlation functions and in the Fourier transforms, and which are endemic of the semi-classical regular orbits in the square quantum dots. Crucial to this result is the excitation of the ballistic dots by quantum point contacts, as the latter provide a collimated excitation of the particles within the dot. This collimation provides a specific excitation of quantum structure related to the semi-classical orbits.

As shown above in figure 1, the dots can be formed in several ways. In all cases, the dot size is much smaller than the elastic mean free path, so that the underlying motion is ballistic in nature. These three structures include: (1) GaAs/AlGaAs heterostructures with surface Schottky barrier gates to define the dots, (2) GaAs/AlGaAs or InGaAs/GaAs heterostructures with in-plane gates to define the dots, and (3) GaAs/AlGaAs heterostructures which have been etched to define the dots. Hence, two different material systems and three distinct gate technologies have been involved in the samples studied. The basic observations are similar in all three cases, and independent of the material system and gate technology. Here, however, we will concentrate on dots of the first sort. For these dots, the gate regions are defined by lift-off of metallic Schottky barrier metals. The dots are basically square in nature, and sizes ranged from 1.0 to 0.4 μm (the electrical sizes are somewhat smaller due to edge depletion around the gates). In nearly all cases studied, the carrier density was 3–5 $\times$ 10^{11} cm^{-2}, and mobilities are typically 40–200 m^2 V^{-1} s^{-1}. The gate design allowed electrons to be trapped in the central square cavity. Measurements were typically carried out at 10–30 mK base temperature in the refrigerator, and source–drain excitation was kept well below the thermal voltage with lock-in techniques utilized.

3.1. Magneto-transport

In figure 2, magneto-conductance traces for a typical sample are shown. Reproducible fluctuations persist across a wide range of magnetic field. At higher magnetic fields, a transition into edge-state behaviour and the quantum Hall effect occurs. At still higher magnetic fields, Aharonov–Bohm oscillations from edge state interference within the dot is observed, and this allows us to unambiguously determine the electrical size of the ballistic cavity. It is found that the basic nature of the reproducible fluctuations is independent of the details of the sample material and gate technology. Instead, this behaviour seems to be a basic property of the dot geometry and size, a result of the *intrinsic* dot properties and quite distinct from the generic results of chaos theory [20]. Here, the basic oscillatory properties are universal, although the specific frequency content is very dot dependent. We will discuss below how these oscillatory

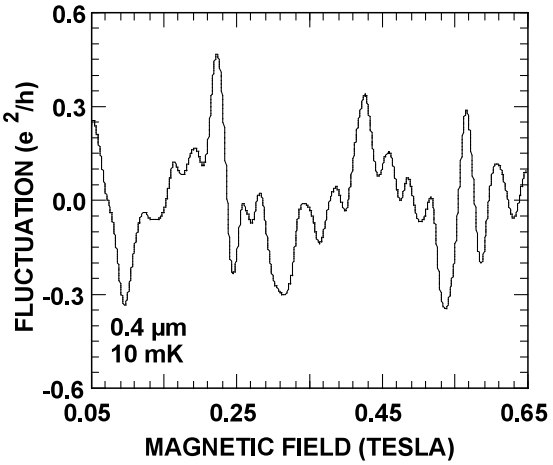

Figure 2. Fluctuations in a 0.4 μm GaAs/AlGaAs quantum dot whose configuration is that of the left picture in figure 1 [21]. The background magneto-resistance has been subtracted to reveal the nature of the quasi-periodic signal.

features of the magneto-conductance are related to the fluctuations in the density of states that arise from the regular, quasi-periodic orbits of the quantum dot itself, and are therefore a reflection of the intrinsic properties of the dots.

Although not evident in these figures, the low field magnetoresistance often exhibits a peak, which is unrelated to weak localization but instead is an intrinsic property of the states within the dot [22]. The actual lineshape of this peak is found to vary with contact opening, and similar behaviour has been observed in simple quantum point contact structures which cannot support chaotic behaviour. Thus, it is improper to assume *a priori* that such peaks are connected with chaotic behaviour. Indeed, phase-space filling can easily be generated by the *integrable* motion within these dots due to the magnetic field induced precession of the orbits. Thus, it is not surprising that the quasi-periodic fluctuations observed in the magneto-conductance are quite different from those observed in chaotic dots.

We have carried out calculations to simulate the behaviour of these dots, using a stable variant of the transfer matrix approach [23]. For example, conductance fluctuations as a function of magnetic field are studied for a 0.3 μm square dot (this size reflects the electrical size, which is less than the actual structure due to gate depletion) with 0.04 μm port openings, which allow two modes to enter and exit the dot. Instead of a random aperiodic variation with magnetic field, a series of nearly periodic oscillations is evident, as may be seen in figure 3. Also apparent are several resonance features. In particular, a set of resonances occurs at $B \sim 0.069, 0.173, 0.283$ and 0.397 T, in which the wavefunction is heavily 'scarred', in that the quantum mechanical amplitude appears to follow a single underlying classical orbit, as shown in figure 4. Given the period for the reappearance of the diamond is $\Delta B \sim 0.11$ T, and using the criterion familiar from the Aharonov–Bohm effect, that $\Delta\phi/\phi_0 = 2\pi$ for the difference in magnetic flux, one obtains $A \sim 0.04\ \mu\text{m}^2$ for the enclosed area, which corresponds well with the enclosed area of the diamond-shaped wavefunction, depicted in figure 3, where the darker areas are points of higher wavefunction amplitude.

Periodic orbits have played a large theoretical role in the computation of semi-classical quantization of bound states for many years, dating to the Einstein–Brillouin–Keller view of quantization. More recent studies indicate that the 'imprints' of these orbits persist up through

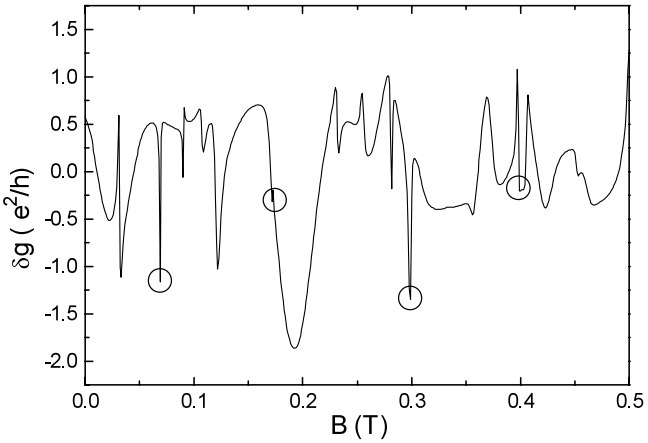

Figure 3. The computed conductance fluctuations at $T = 0$ K for a 0.3 μm dot. The circles indicate the periodic resonances which display the heavily scarred wavefunction of figure 4.

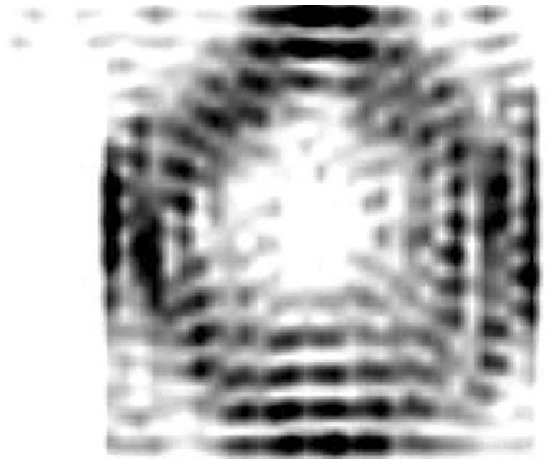

Figure 4. The squared magnitude of the wavefunction as a function of position within the dot [23]. Darker shading corresponds to higher amplitude. The picture correspond to the dot with 0.04 μm openings at $B = 0.173$ T.

thousands of states [24], a result that suggests the closed orbits are quite stable in regular systems and only become unstable as one passes to the ergodic regime, which seems to be replicated as one passes from the semi-classical to the quantum regime. The quantum point contact imposes a boundary condition on the particles, in which the entry angle is determined by the wave mechanical nature of propagation through the quantum point contact. It is this collimation that is important for exciting a particular set of regular orbits of the particles. From the study of classical orbits in these dots, we can compute the transmission, and hence the conductance, as well as the fluctuations. In figure 5, we compare the Fourier transform of the fluctuations for the three cases of (a) the experiment, (b) the quantum simulation, and (c) a classical simulation. Clearly, the strong agreement between these three frequency plots supports the importance of the regular orbits on the quantization of the ballistic dots. It may be seen that there is a strong main peak at 9 T^{-1}, which corresponds to the periodicity of the

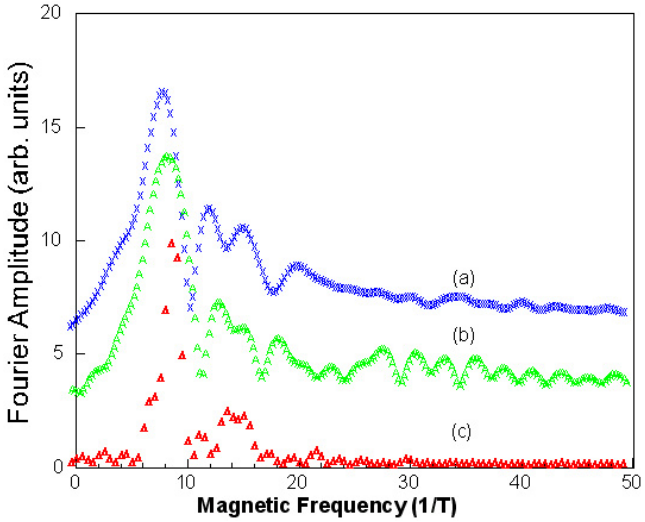

Figure 5. A comparison of the spectra of the correlation functions for the experimental dot (a), the classical billiard (b), and the quantum simulation (c), all for an effective dot size of 0.3 μm [23]. The curves are offset for clarity.

scarred diamond-shaped wavefunctions of figure 4. In addition, there are higher harmonics, and some other frequencies observed in the spectrum. These harmonics are related to orbits which are more complicated.

In figure 6, we plot the conductance calculated for an open square dot with four propagating modes in the quantum point contact leads. As mentioned above, the conductance is computed with a stabilized version of the transfer matrix approach and hard wall potentials [23]. In this particular case, we have used hard wall boundaries; using a self-consistent potential with soft walls softens the sharp resonances and leads to fluctuations more in line with that found experimentally, but does not change the basic structure (this has been discussed in detail in [25]). The lighter areas correspond to higher values of the conductance, while darker areas correspond to higher values of the resistance. There are structured lines in the conductance which are reminiscent of the energy levels in the Darwin–Fock spectra [26]. Moreover, it is clear that the magnetic field indeed splits degeneracies which exist in the absence of this field. The diagonal lines seem to be uniformly separated, and provide direct evidence for 'closed' orbits, as the scars of figure 4 occur along these lines. This periodicity is thus thought to be the cause of the periodic scars that are observed in the wavefunctions for these structures. One might at first glance be led to believe that these highly structured conductances are unique to the square geometry studied here, but they have been found in stadium structures [7] and in more re-entrant structures where careful coupling of the Schödinger/Poisson solution derived potential with the quantum simulations reproduce the experimentally observed behaviour [27]. But we also note that the periodicity exists as one varies the Fermi energy, such as will occur when the gate voltage is varied. We turn to this next.

3.2. Gate-induced fluctuations

The results found in these dots, as the gate voltage is varied, are quite similar in behaviour to that seen as the magnetic field is varied. As the gate voltage is made more negative, the dot is reduced in size and the various energy levels are pushed up through the Fermi energy.

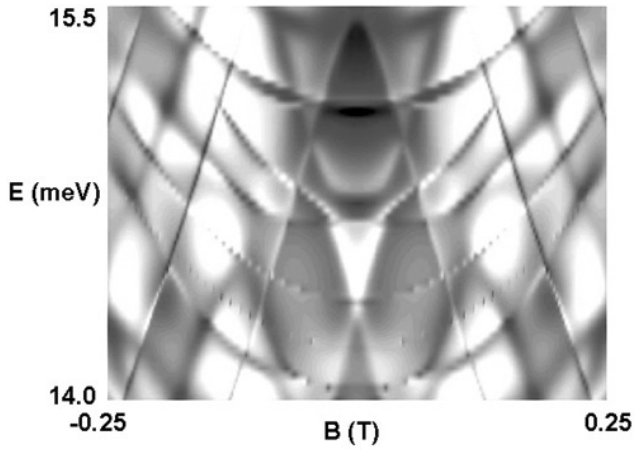

Figure 6. The calculated conductance spectrum through a 0.3 μm dot. The lighter areas represent higher conductance, the darker areas lower conductance.

This leads to a series of conductance oscillations, which ride on top of a monotonic background, and which disappear at a few kelvins. It is important to note that these oscillations are not the universal conductance oscillations often attributed to mesoscopic systems. The latter typically arise from (impurity induced) disorder within the system, and are aperiodic. To the contrary, the oscillations we find become stronger in high quality material with less disorder and exhibit one, or perhaps two, dominant frequencies which are dot-size dependent. When the gate voltage is varied, the actual frequency depends upon both the dot size and the lever arm from the gate voltage to the actual Fermi level motion within the dot. The oscillations often are observed over the entire range of gate voltage and persist to conductance values of 15 e^2/h, which represents a very open dot. Again, the experimental results and quantum simulations (discussed below) yield the same dominant frequency in the dots. Here, we will focus upon a smaller dot, whose gate defined dimension varied from 0.2–0.3 μm, depending upon the value of the applied gate voltage. In figure 7, we plot the conductance through the quantum dot as the gate voltage is varied. It may be seen that the fluctuations ride on a uniformly increasing (for increasing gate voltage) conductance background. Rather than try to smooth the curve, the temperature is raised above 2 K, a point at which the fluctuations are largely damped out. This curve is then subtracted from the low temperature curve to isolate the fluctuations themselves, which are plotted as the upper trace in figure 8. These oscillations are very nearly periodic with a dominant period of about 15 V^{-1}.

To account for the behaviour seen in the experiment, we have used our recursive scattering matrix simulation to study these fluctuations. These begin by first computing the exact self-consistent potential for the dot at more than 300 gate voltages. This is accomplished with a three-dimensional Poisson solver, which uses only experimental values for the various parameters of the heterostructure and gate layout. Once the potential profile is known, we simulate the quantum transport through the device. The calculations are performed for a fixed Fermi level which is defined by its value in the reservoirs to which the dot is attached through the quantum point contacts. The influence of these contacts is included via the exact potential profile of the *open* dots. This approach also allows computation of the wavefunction within the dot. This latter can be decomposed into the states of the closed dot for later use (discussed below) by an eigenfunction decomposition. The computed conductance fluctuation is also shown in figure 8 as the lower trace. While there is a variation in amplitude, the frequency

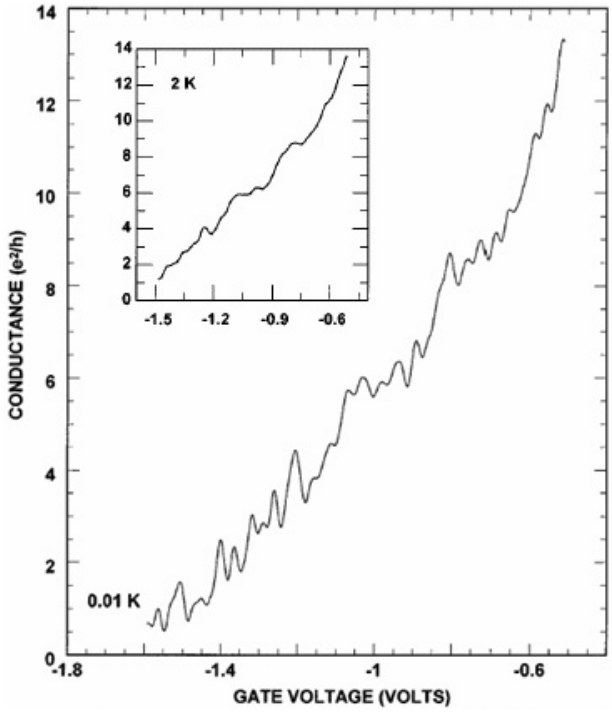

Figure 7. The conductance through a 0.3 μm dot as the gate voltage is varied [28]. The inset shows the conductance when the temperature is raised to 2 K, and this is used to remove the background conductance.

and general periodicity agree quite well between the experiment and theory. This may be confirmed by comparing the Fourier transforms of these traces, and this is shown in figure 9.

The same self-consistent potential has also been used to study the classical dynamics of electrons injected into these dots [29]. As with most systems of this nature, the dynamics is non-hyperbolic in that there are regions of chaotic scattering which coexist with non-escaping KAM islands surrounding stable orbits in phase space. Hence, these dots have a mixed phase space [30]. As mentioned above, when the quasi-periodic fluctuations are removed by averaging over gate voltage, only the chaotic background remains. It may be presumed that this chaotic sea provides the background conductance through the dot, such as that shown in the inset to figure 7, and to provide the regions of chaotic scattering seen in the phase space portraits of the classical dynamics within these dots [29]. Hence, the periodic orbits which are enclosed within the KAM island must correspond to the quasi-periodic fluctuations that we have been describing here. This was checked by varying the gate voltage, and observing the change in size of these periodic orbits. The results indicate that this periodicity agrees exceedingly well with that found for both the experiment and the quantum simulation. The conclusion is that it is those scarred quantum wavefunctions, which give rise to the periodicity, that relax into the classical periodic orbits on the KAM island. This is important, as it is generally felt that the pointer states are essentially the classical remains of the quantum states.

4. Pointer states

As indicated above, we have coupled the experiments to detailed simulations. These simulations begin by computing the three-dimensional, self-consistent potential profile

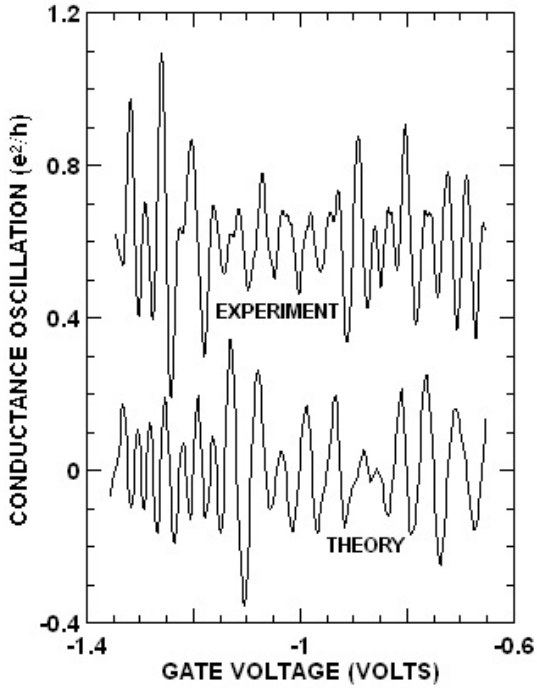

Figure 8. The conductance fluctuations, top trace, are compared with those calculated from the recursive scattering matrix simulation [28].

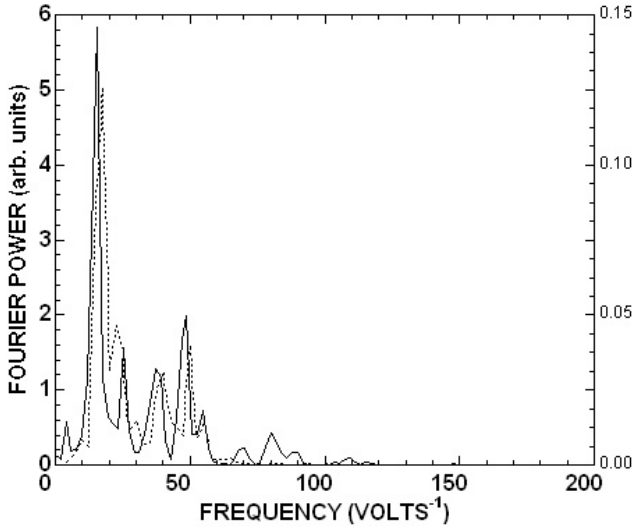

Figure 9. Spectral density for the experiment (solid curve) and the simulation (dashed curve) [28].

of the open dot at each gate voltage, from which the conductance is computed using a lattice discretization of the single-particle Schrödinger equation in the effective mass approximation [23]. Here, the open dot is broken into a set of slices across which we translate using a stable, iterative scattering matrix approach. In this way, we can obtain the conductance

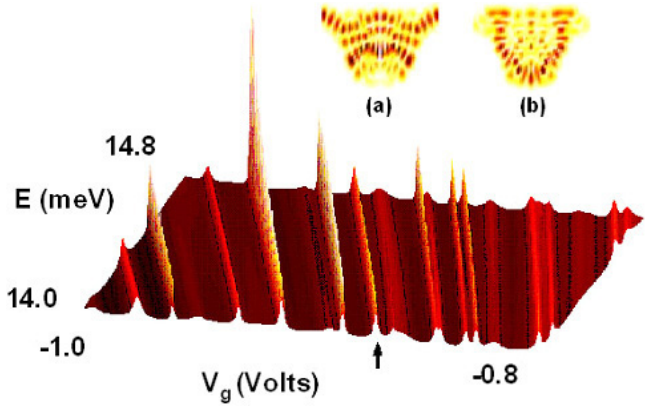

Figure 10. The density-of-states peaks, corresponding to conductance resonances, in the quantum dot [17]. The peaks correspond to the stable wavefunctions in the dot as the gate voltage and Fermi energy are varied. As the gate voltage is varied, the dot becomes more open, but the stable resonances show no increase in width as the coupling to the environment is increased. The arrow indicates a resonance, whose wavefunction is indicated by inset (b), for which the state of inset (a) is quite near, but is completely damped. The linewidth is about 21 μeV.

from the Landauer formula. Finite temperature is included by averaging the conductance traces over an energy range of $k_B T$ with the Fermi function. From these simulations, conductance oscillations are found which agree well with those observed in experiment. In particular, both the number of Fourier peaks which occur in the simulation and their amplitude agree well with the experimental results, as was seen in figures 5 and 9. From studies of the wavefunction itself, we find that these peaks correspond to the frequencies at which specific sets of scarred wavefunctions recur in the dot. Decomposition of these scarred wavefunctions show that they arise from a single eigenstate of the closed, but 'extended' dot. Whether closed or open, this extended dot is a 'perturbed' quantum dot. The cavity itself is augmented by attaching perturbing QPCs, usually in a manner that breaks the horizontal symmetry. In previous studies comparing open and closed dots [9], we have found that it is vitally important that at least a portion of the QPC be included as part of the closed system, as it gives rise to a non-trivial perturbation to the system that cannot be neglected.

The scarred states are quite stable as the leads are opened to allow stronger coupling to the environment, and in fact seem to be insensitive to this coupling, which agrees with experiments which have demonstrated that the dominant frequency components of the conductance oscillations are extremely stable to variation of the coupling strength over a wide range. Indeed, we have even observed evidence for these regular oscillations in dots whose leads support as many as 30 propagating modes. In figure 10, we show the density of states within a 0.3 μm dot. This is dominated by conductance resonances that move as the bias is varied, the latter of which changes the coupling to the environment as well as the dot size. It may be seen that the linewidth does not change significantly as the environmental coupling is increased, even though the resonance is shifted due to the change in the dot size. Indeed, nearby states are completely damped by the environment and uncoupled to the stable state, even though they may be separated by an energy much less than the linewidth (approximately 21 μeV in the figure). For example, the resonance indicated by the arrow in this figure has another closed-dot eigenstate nearby, which is completely damped by its interaction with the environment, so no peak appears in this figure. The wavefunction of the resonance is shown in inset (b), while the nearby state is shown in inset (a).

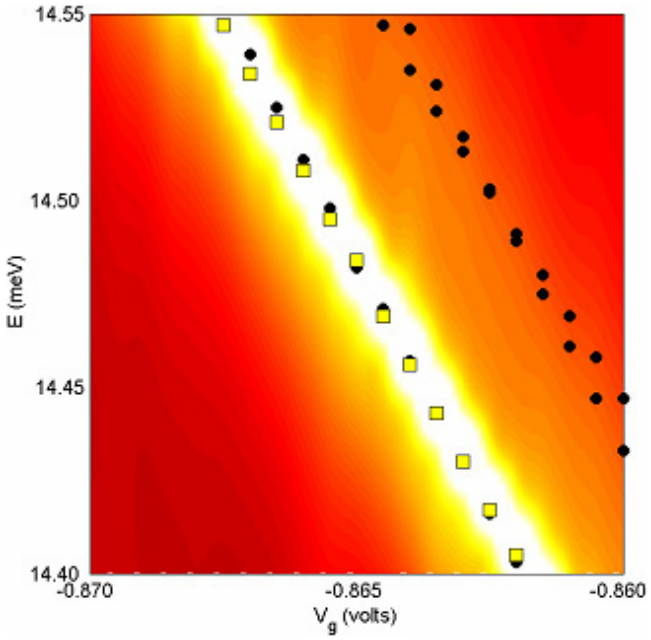

Figure 11. An enlargement of a portion of figure 10 to show the lack of interaction between the stable wavefunctions and nearby states [17]. The dark regions are those of lower amplitude in the density of states. The (colour) filled squares are the stable resonance indicated by the arrow in figure 10 and the wavefunction of inset (b) to that figure. The black circles are nearby states, which are completely damped by the interaction with the environment.

We illustrate the lack of coupling to nearby states further in figure 11. Here, we expand a portion of figure 10, and the darkness of the image relates to the amplitude of the density of states. The filled squares are the robust conduction states of figure 10(b), while the black circles are nearby states that are completely damped by their interaction with the environment. While one of these actually crosses the resonant state, there is no interaction as the two wavefunctions are orthogonal, as may be seen from the wavefunctions in the insets to figure 10. This orthogonality between the pointer state and the nearby state is evident, and presumed to result from the einselection process, where the density matrix becomes diagonal in the pointer states. Decoherence of the other states arises from their strong interaction with the environment, and any excitation of these states results in amplitude leakage to the environment. In a closed system, these background states would also be excited, but they are damped in the open system. We interpret these as contributing to the background conductance, which clearly increases with the degree of opening in the quantum dots, which is further discussed below.

As mentioned above, we have found that the pointer states tend to be scarred by remnants of classical periodic orbits, suggesting that these are the route through which the quantum-to-classical transition occurs. Now, we turn to a discussion of how the process of einselection is reflected in the statistical properties of the energy levels of these open quantum dots, in particular of the pointer states that survive when the dot is open to its environment. These properties have been studied previously in experiments on quantum dots [5, 31] and microwave cavities [32]. The relationship between the classical dynamics of a system and the spectral statistics of its quantum analogue has been a primary concern in the study of quantum chaos [33, 34]. Systems with integrable dynamics are expected to have uncorrelated energy

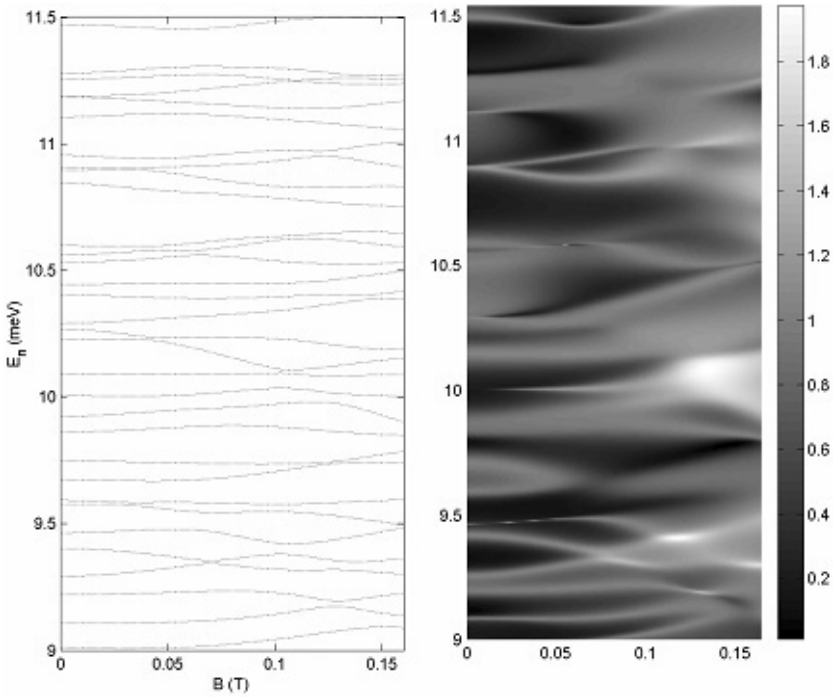

Figure 12. (a) Eigenenergies as a function of the magnetic field. (b) The corresponding conductance through the dot.

levels that yield Poisson statistics, while completely chaotic dynamics is associated with the Wigner statistics of one of the random matrix ensembles: the Gaussian orthogonal ensemble (GOE) when time reversal symmetry is preserved and the Gaussian unitary ensemble (GUE) when it is broken. Here we show that, when the stadium is opened to the environment and only the pointer states with amplitude localized to in the interior remain, there is a dramatic and profound change in the level distribution. The distribution of pointer states becomes Poissonian, indicating that these are intimately associated with the regular orbits, which normally have zero measure in the classically chaotic system. Here, we continue to deal with our nominally rectangular quantum dots, but we show elsewhere that this behaviour is also found in stadium dots which are normally considered to be fully chaotic in their classical behaviour [35].

In figure 12(a), we show a series of eigenvalues of the perturbed stadium with energies in the range 9 meV $\leqslant E_n \leqslant$ 11.5 meV, as the magnetic field (B) is varied up to 0.16 T. These are computed for a gate voltage of -0.8 V, and were computed by solving the same lattice discretized version of the single-particle two-dimensional Schrödinger equation in the effective mass approximation discussed above. In figure 12(b), we show the conductance that is obtained from the transmission coefficients of the modes via the Landauer formula. For our analysis of the spectral statistics of this quantum dot, we have considered states in this energy range, so that there are a number of propagating modes in the QPCs in each case. Since only a limited number of eigenstates occur over this range, we have varied the perpendicular magnetic field (0.0 T $\leqslant B \leqslant$ 0.16 T, in 0.001 T steps) to generate many different ensembles of eigenstates, thus greatly increasing the number of energy levels available for the analysis. The number of QPC modes does not vary over this range of field. Moreover, the values used

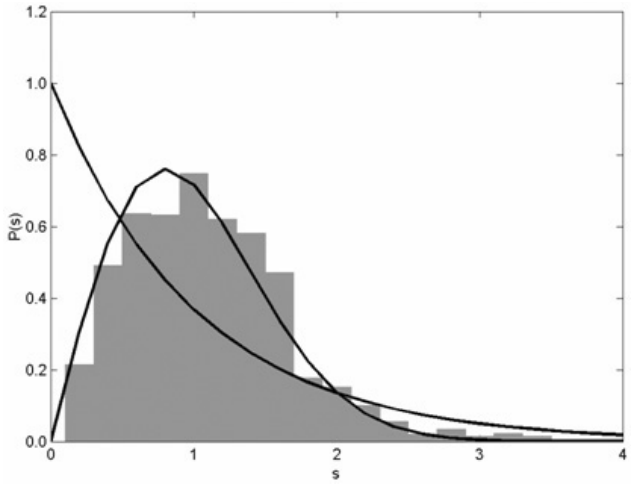

Figure 13. The level spacing distribution for *all* perturbed stadium eigenstates found in the range 9 meV $\leqslant E_n \leqslant$ 11.5 meV and 0 T $\leqslant B \leqslant$ 0.16 T. For comparison, the Poisson and GOE distributions are also plotted.

for B are small enough so that no substantial change in the nature of the electron dynamics is expected.

As is customary, before performing the statistical analysis of the level spacings, we have mapped the raw energy levels, $\{E_i\}$, onto a dimensionless, *unfolded* set of eigenvalues, $\{\varepsilon_i\}$, which have a local density of unity [36]. This is achieved in the present case by replacing the raw eigenvalues with $\varepsilon_i(B) = E_i(B)/\overline{\Delta E}$, where $\overline{\Delta E}$ is the average level spacing for a given magnetic field, taken over the energy window described above. This yields a dimensionless sequence of nearest-neighbour energy level spacings $\{s_i = \varepsilon_{i+1} - \varepsilon_i\}$ for each value of B. Figure 13 shows the unfolded nearest neighbour spacing distribution, $P(s)$, for the *entire set* of energy levels. For comparison, we have also plotted the Poisson ($P_{\rm P}(s) = {\rm e}^{-s}$) and GOE ($P_{\rm GOE}(s) = (\pi s/2)\exp(-\pi s^2/4)$) distributions. Clearly, the closest agreement is with the GOE distribution. On the surface, this is a surprising result, since applying a magnetic field breaks time reversal symmetry, which usually favours the GUE distribution. However, in the present case, the symmetry breaking usually provided by the field is negated by the fact that our perturbed dot has vertical symmetry, so that the states for $-B$ are equivalent mirror images of those with $+B$. Moreover, the transition from GOE to GUE, with magnetic field is not expected to be abrupt [37].

In figure 14, we plot $P(s)$ for the pointer states only. Remarkably, $P(s)$ *for pointer states very clearly follows the Poisson distribution*. By opening the perturbed cavity, it is as if we have forced it to make a transition from classically *chaotic* to classically *regular* behaviour. While this may seem a surprising result, it is actually quite reasonable, given that we have found that the pointer states have wavefunctions that are strongly scarred by periodic orbits. In a stadium billiard in the classical limit, these orbits are, of course, well known to all be unstable, and to have zero measure. In our nearly rectangular quantum dot, the classical orbits are normally expected to be regular, although this is not really the case when we see that GOE statistics result for all eigenstates. By opening the billiard to the environment, however, our analysis shows that the pointer states now dominate the properties of the quantum system. A GOE-like distribution can be recovered in the case of pointer states but only if *tunnelling* barriers are placed over the QPCs so that the conductance is reduced to well below e^2/h.

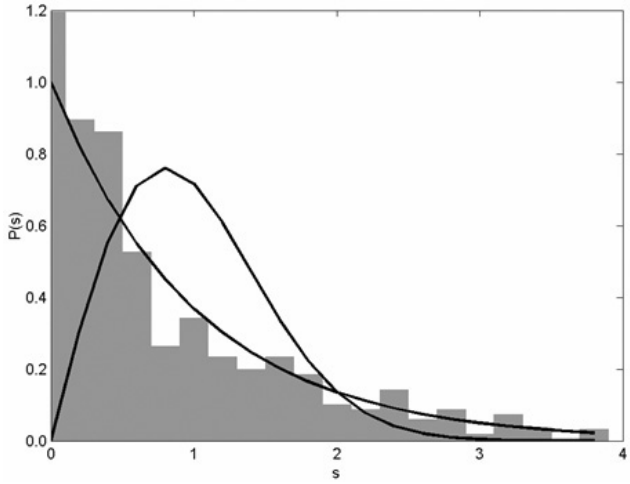

Figure 14. As in figure 13, but in this case the level spacing distribution is for pointer states only.

It should be mentioned that it is usual in these sorts of calculations to either study a cavity that is strongly asymmetric (the quarter stadium being a canonical example) or to segregate eigenstates according to their parity, in order to remove the possibility of correlations *a priori*. This is something we have not explicitly done. Thus, despite the fact that we have not removed any correlations by hand, we find that the pointer states can yield something very close to the *uncorrelated* Poisson distribution. As it turns out, even for the closed dot case, the perturbing effect of having attached QPC segments automatically eliminates many of the correlations that would otherwise occur if we were considering a standard full stadium. This is why the $P(s)$ for all the eigenstates can fall essentially on top of the GOE distribution in figure 13.

5. Phase breaking

As we have discussed above, the classical dynamics of these open dots exhibits a mixed phase space behaviour. A Poincaré section taken normal to the plane of the dot, and passing through the point contacts, exhibits the characteristic sea of chaos and a stable KAM island of orbits which correlate well with the observed gate voltage dependence and with the scarred wavefunctions. The orbits on the KAM island are isolated from the leads and must be coupled to the environment by phase space tunnelling. The states on the KAM island exhibit exactly the same periodicity as the stable quantum states discussed above, and these clearly correspond to one another as expected from the einselection theory [14]. It is this process that takes the quantum states and then correlates them well with what become the classical orbits. On the other hand, the KAM islands are surrounded by a 'sea of chaos', which corresponds to the background states which are strongly coupled to the environment, and thus heavily damped. The occupation of these latter states is lost to the environment as the dot is opened, as they no longer possess any amplitude localized within the dot. The strong decoherence of these states leads to the destruction of their quantum nature and their contribution to the chaotic states yielding the background conductance in the dot. Ultimately, the pointer states have to decohere as well, and within the einselection theory, this should also be done through coupling with the environment.

One of the key parameters for the observation of quantum interference effects in mesoscopic systems is the phase-breaking time τ_ϕ. In addition to internal processes, the

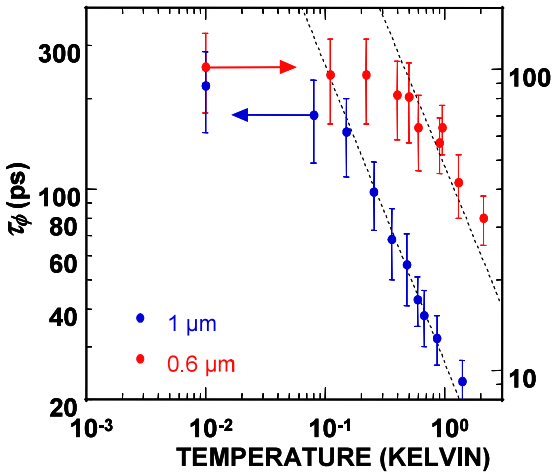

Figure 15. The variation in the measured phase breaking time in two different quantum dots [43]. The dotted line is a guide to the eye indicating a slope of $1/T$.

coupling of a quantum system to its environment causes phase randomization of the electron wavefunction, as discussed above. There have been many measurements of this important phase-breaking time in diffusive mesoscopic structures, such as quasi-two-dimensional systems and quantum wires [38]. However, there have been relatively few studies of phase breaking in quantum dots, which some believe to be zero-dimensional systems.

In this section, we will discuss the phase breaking time measurements that we have carried out on these dots. Generally, these are characterized by two distinct behaviours. At low temperatures, the phase breaking time is independent of temperature, a result generally in keeping with our understanding of the electron–electron interaction in mesoscopic systems [39]. At high temperatures, however, the phase breaking time decreases as a power of the temperature, with the exponent being related to the dimensionality of the system. Here, we show that, if the dot is coupled to a large two-dimensional system, this power law is T^{-1}. However, if the dot is coupled to one dimensional wires at each QPC, the power law appears to have the form $T^{-2/3}$. These results are also consistent with the understanding of the electron–electron interaction in mesoscopic systems [40]. Thus, this high temperature decay seems to indicate that the phase breaking process for the conductance oscillations, which arise from the pointer states, is characterized by the dimensionality of the environment to which the quantum dot is directly attached.

In figure 15, the dependence of the phase breaking time for two dots whose lithographic dimensions are 0.6 and 1.0 μm, is shown. The shape of the dot is that of the left panel of figure 1. The phase-breaking time was determined by measuring the magnetic-field dependence of the correlation magnetic field for the fluctuations in the magnetoconductance [41], a technique shown to give good values for this important parameter [42]. As mentioned, the measurements indicate a saturation in the phase-breaking time below a transition temperature, which is sample size dependent, and a decay at higher temperatures. This saturation at low temperatures is not due to a saturation of the sample temperature, as the amplitude of the conductance oscillations continue to increase as the temperature is lowered. This saturation also occurs in other dimensions as well, although the temperature decay portion has a different exponent for different dimensionality [40]. In the figure, the temperature decay is as T^{-1}, which is indicative of a two-dimensional system. From figure 1 it is clear that the dot is connected

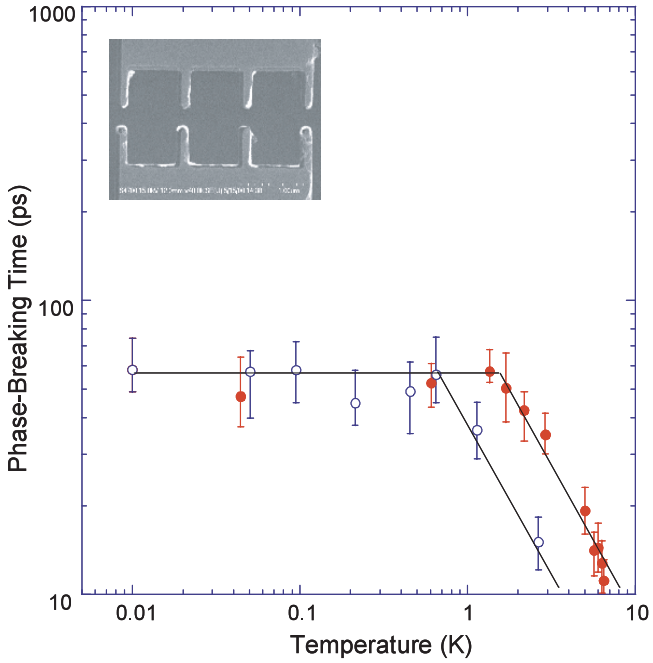

Figure 16. The phase breaking time for a three dot (open circles) and a four dot array (closed circles) [45]. The three dot array is shown in the inset.

to regions which behave as quasi-two-dimensional electron gases, and here the temperature decay appears to correspond to that nature.

Surprisingly, this behaviour persists even when multiple dots are coupled together. This can be shown by actually measuring the phase breaking time in dot arrays. The two arrays discussed here are composed of three (four) identical dots in series, separated by evenly spaced quantum point contacts. The lithographic dimensions of the dots were $1.4 \times 1.0\ \mu\text{m}^2$ ($1.0 \times 0.6\ \mu\text{m}^2$), which is non-square [44]. The structures were designed using the split-gate technique and all gates were tied together to provide uniform formation of the dots. The three dot array is shown in the inset to figure 16. Measurements were performed in magnetic fields up to 4 T. In general, a very low sample current was used except for the non-equilibrium studies, for which the current was varied from 50 pA to 130 nA. The phase-breaking time as a function of the lattice temperature is shown in the main panel of figure 16 for the two dot arrays. Once again, the temperature decay seems to vary as T^{-1}, in keeping with the fact that the arrays are embedded in a quasi-two-dimensional electron gas. The pointer states apparently do not significantly decohere within one dot or the dot array, but this decoherence occurs within the environment as represented by this quasi-two-dimensional contact system. This is a very interesting result, and is in agreement with studies which have shown that the fluctuations themselves can be composed of orbits which are coherent across the dots of the array [45]. Indeed, there is some indication in figure 16, that the phase-breaking time is longer in the four dot array than in the three dot array. As these two devices were made on the same sample, at the same time, this observation may be valid, although much more work in this area needs to be done before such a conclusion can be drawn.

We now turn to the observation of the phase breaking time in an open quantum dot which is mediated by the point contact leads, and *coupled to quantum wires*. The gated dot is defined

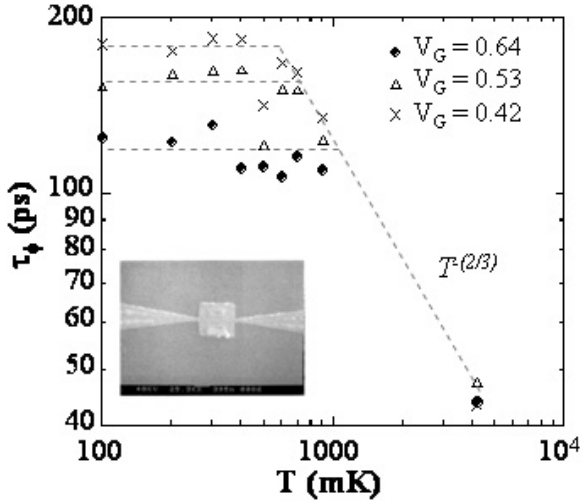

Figure 17. The phase breaking time in a single etched dot, which is attached to quantum wires [46]. Here the coupling is varied as the gate voltage is made more negative, which increases the phase breaking time in the saturation regime. A photo micrograph of the dot and wires is shown in the inset.

by electron beam lithography and etching to be 0.8 μm square with ∼150 nm quantum point contact leads positioned at either side. These leads open to quantum wires which gradually increase in width to 2 μm, over a distance of 10 μm, before reaching a two-dimensional electron gas patterned into a Hall bar structure (the device structure is shown in the inset in figure 17). The wires provide adiabatic coupling to the dot. The saturated phase breaking time, at low temperature, is found to depend on the nature of the coupling between the dot and the wire, as this is varied by changing the bias applied to a top gate on the structure. At higher temperatures, the phase breaking time is found to exhibit an apparent $T^{-2/3}$ behaviour [46], which is consistent with the coupling of the dot to a one-dimensional quantum wire [39, 40], as shown in figure 17. However, some caution is advised as only a few data points are present. These suggest that the behaviour has this shape, but much more work is necessary to confirm this. As we discussed above, one expects to have the $T^{-2/3}$ behaviour for phase breaking processes in a one dimensional system. Once again, we seem to see that the decoherence of the pointer states is occurring in the environmental system to which the quantum dot is coupled.

6. Conclusions

In summary, we find that conductance oscillations in open quantum dots are related to a set of eigenstates, whose stability is consistent with einselection; i.e. the selection of a set of *discrete pointer states* which are quite stable as the coupling to the environment is increased. The observed pointer states have a narrow line width, and their superposition with nearby quantum states, well coupled to the environment, is heavily damped by decoherence. Moreover, the scarred wavefunctions of the pointer states strongly resemble the trajectories found in classical simulations of the same self-consistent potential, which suggests these are the route through which the quantum to classical transition occurs. This latter is supported by studies which show that pointer states in an open stadium quantum dot can yield Poisson spectral statistics associated with such classically regular behaviour even though the eigenstates of the

corresponding closed system follow the GOE distribution associated with chaos. It should be mentioned that there have been previous theoretical spectral studies on quantum dots that did not observe such a change in behaviour [47]. A key factor that enabled us to see this dramatic shift from a chaotic distribution to a regular one in our calculations is that we studied very open quantum dots strongly coupled to the external environment, as opposed to the comparatively weakly coupled dots considered previously. By strongly coupled we mean that, not only are the QPCs large enough to support several propagating modes, but they are large enough in comparison to the size of dot to have a very significant effect on the nature of the confinement. Specifically, we have ensured that the pointer states that survive are localized in the interior of the dot, states that are typically scarred by relatively simple periodic orbits. As we have shown, the GOE distribution can be recovered in the spectral statistics of the total states in the system, but only when finite potential barriers are placed over the QPCs so that transmission occurs only via tunnelling and the interaction with the environment is almost completely suppressed. Even here, however, the states that become the pointer states continue to have Poissonian statistics.

The view that these are proper pointer states is also supported by measurements of the phase breaking time of these states. This exhibits a temperature independent region at low temperatures, but also a temperature decay as a power law at higher temperatures. The power law seems to be indicative of the environment to which the dot is coupled, particularly characterizing the dimensionality of this environment. The fact that the decoherence is occurring in the environment, and not in the dot, is that coupled dot arrays seem to yield higher values of the phase breaking time; e.g., more robust behaviour as the temperature is raised.

From these studies, we feel that the conductance oscillations that occur in open quantum dots are indeed a manifestation of the einselection process and the occurrence of pointer states within the dot. These govern the transition from the pure quantum system to the essentially classical system which appears in measurements.

Acknowledgments

The work described here has been supported by the Office of Naval Research, The Department of Energy, and the National Science Foundation. The authors have enjoyed helpful discussions from a great many people, who are too numerous to list individually.

References

[1] See, e.g. Bimberg D, Grundmann M and Ledentsov N N 1999 *Quantum Dot Heterostructures* (Chichester: Wiley) and references therein
[2] Reed M A, Randall J N, Luscombe J H, Frensley W R, Aggarwal R J, Matyi R J, Moore T M and Wetsel A E 1988 *Phys. Rev. Lett.* **60** 535
[3] McEuen P L, Foxman E B, Meirav U, Kastner M A, Meir Y and Wingreen N S 1991 *Phys. Rev. Lett.* **66** 1926
[4] Jalabert R A, Baranger H U and Stone A D 1988 *Phys. Rev. Lett.* **60** 477
[5] Marcus C M, Rimberg A J, Westervelt R M, Hopkins P F and Gossard A C 1992 *Phys. Rev. Lett.* **69** 506
[6] Chang A M, Baranger H U, Pfeiffer L N and West K W 1993 *Phys. Rev. Lett.* **70** 3876
[7] Akis R, Ferry D K and Bird J P 1997 *Phys. Rev. Lett.* **79** 123
[8] Akis R, Bird J P, Ferry D K and Vasileska D 2000 *Physica* E **7** 745
[9] Akis R, Bird J P and Ferry D K 2002 *Appl. Phys. Lett.* **81** 129
[10] Nazmitdinov R G, Pitchugin K N, Rotter I and Šeba P 2003 *Phys. Rev.* B **66** 085322
[11] Wheeler J A and Zurek W H (ed) 1983 *Quantum Theory and Measurement* (Princeton, NJ: Princeton University Press)
[12] See, e.g. the recent review Zurek W H 2003 *Rev. Mod. Phys.* **75** 715

[13] Zurek W H 1982 *Phys. Rev.* D **26** 1862
[14] Zurek W H 1981 *Phys. Rev.* D **24** 1516
[15] Eisert J 2004 *Phys. Rev. Lett.* **92** 210401
[16] Blanchard Ph and Olkiewicz R 2003 *Phys. Rev. Lett.* **90** 010403
[17] Ferry D K, Akis R and Bird J P 2004 *Phys. Rev. Lett.* **93** 026803
[18] Connolly K, Pivin D P Jr, Ferry D K and Wieder H H 1996 *Superlatt. Microstruct.* **20** 307
[19] Bird J P, Ishibashi K, Aoyagi Y, Sugano T and Ochiai Y 1994 *Phys. Rev.* B **50** R18678
[20] Bird J P, Akis R, Ferry D K, de Moura A P S, Lai Y-C and Indlekofer K M 2003 *Rep. Prog. Phys.* **66** 583
[21] Bird J P, Akis R, Ferry D K, Aoyagi Y and Sugano T 1997 *J. Phys.: Condens. Matter* **9** 5935
[22] Akis R, Vasileska D, Ferry D K and Bird J P 1999 *Japan. J. Appl. Phys.* **38** 328
[23] Akis R, Ferry D K and Bird J P 1996 *Phys. Rev.* B **54** 17705
[24] Berry M V 1989 *Proc. R. Soc.* A **423** 249
[25] Akis R, Bird J P, Vasileska D, Ferry D K, de Moura A P S and Lai Y-C 2003 *Electron Transport in Quantum Dots* ed J P Bird (Boston, MA: Kluwer–Academic) pp 209–76
[26] Ferry D K 1995 *Quantum Mechanics* (Bristol: Institute of Physics Publishing) p 208
[27] Okubo Y, Ochiai Y, Vasileska D, Akis R, Ferry D K, Bird J P, Ishibashi K, Aoyagi Y and Sugano T 1997 *Phys. Lett.* A **236** 120
[28] Bird J P, Akis R, Ferry D K, Vasileska D, Cooper J, Aoyagi Y and Sugano T 1999 *Phys. Rev. Lett.* **82** 4691
[29] De Moura A P S, Lai Y-C, Akis R, Bird J P and Ferry D K 2003 *Phys. Rev. Lett.* **88** 236804
[30] Ketzmerick R 1996 *Phys. Rev.* B **54** 10841
[31] Marcus C M, Westervelt R M, Hopkins P F and Gossard A C 1993 *Chaos* **3** 4
[32] Alt H, Dembowski C, Gräf H-D, Hofferbert H, Rehfeld H, Richter A and Schmit C 1999 *Phys. Rev.* E **60** 2851
[33] Stockmann H 1999 *Quantum Chaos, An Introduction* (Cambridge: Cambridge University Press)
[34] Gutzwiller M C 1990 *Chaos in Classical and Quantum Mechanics* (New York: Springer)
[35] Akis R, Ferry D K and Bird J P 2004 submitted
[36] Brody T A, Flores J, French J B, Mello P A, Pandel A and Wong S S M 1981 *Rev. Mod. Phys.* **53** 385
[37] Yan Z and Harris R 1995 *Europhys. Lett.* **32** 437
[38] Lin J J and Bird J P 2002 *J. Phys.: Condens. Matter* **14** R501
[39] Ferry D K 2000 *Semiconductor Transport* (London: Taylor and Francis) pp 355–9
[40] Altshuler B L, Aronov A G and Khmelnitsky D E 1982 *J. Phys. C: Solid State Phys.* **15** 7367
[41] Ferry D K, Edwards G, Yamamoto K, Ochiai Y, Bird J P, Ishibashi K, Aoyagi Y and Sugano T 1995 *Japan. J. Appl. Phys.* **34** 4338
[42] Bird J P, Ishibashi K, Ferry D K, Ochiai Y, Aoyagi Y and Sugano T 1995 *Phys. Rev.* B **51** 18037
[43] Bird J P, Linke H, Cooper J, Micolich A P, Ferry D K, Akis R, Ochiai Y, Taylor R P, Newbury R, Omling P, Aoyagi Y and Sugano T 1997 *Phys. Status Solidi* b **204** 314
[44] Prasad C, Ferry D K, Shailos A, El-Hassan M, Bird J P, Lin L-H, Aoki N, Ochiai Y, Ishibashi K and Aoyagi Y 2000 *Phys. Rev.* B **62** 15356
[45] Elhassan M, Bird J P, Shailos A, Prasad C, Akis R, Ferry D K, Takagaka Y, Lin L-H, Aoki N, Ochiai Y, Ishisbashi K and Aoyagi Y 2001 *Phys. Rev.* B **64** 085325
[46] Pivin D P Jr, Andresen A, Bird J P and Ferry D K 1999 *Phys. Rev. Lett.* **82** 4687
[47] Wang Y, Zhu N, Wang J and Guo H 1996 *Phys. Rev.* B **53** 16408